16TH EUROPEAN CONFERENCE ON EARTHQUAKE ENGINEERING THESSALONIKI 18 - 21 JUNE 2018

THE EFFECT OF THE ANGLE OF SEISMIC INCIDENCE WHEN DEFINING A STATISTICAL MODEL FOR STRUCTURAL DEMAND

Despoina SKOULIDOU[1], Nuno PEREIRA[2], Xavier ROMÃO[3]

ABSTRACT

Probabilistic analyses often require making assumptions concerning the statistical distribution of the variables involved. In this context, the statistical distribution of two demand parameters is examined herein when three-dimensional analysis of RC buildings is performed considering multiple angles of seismic incidence. Six buildings are subjected to multi-stripe analysis with bi-directional ground motion groups of various sizes applied along one to twelve angles of incidence and datasets of demand parameters are collected. Seven statistical models are then fitted to the datasets and their performance is examined based on quantile-quantile plots and the corresponding coefficient of determination. The results show that using more than one angle of seismic incidence doesn't affect the type of demand distribution, unless highly inelastic structural response is achieved. The generalized extreme distribution exhibits a marginally higher fitting performance when compared to that of the lognormal distribution. However, due to the larger variability of the coefficient of determination of the generalized extreme value distribution when small ground motion groups are used, the lognormal distribution is preferred to fit the demand data even when multiple angles of seismic incidence are used.

Keywords: Angle of seismic incidence; probabilistic seismic demand; RC buildings; statistical models; probability distribution fitting

1. INTRODUCTION

Seismic analysis using probabilistic methods has been gaining ground against traditional deterministic methods over the years. The ability to simulate phenomena that are uncertain by nature and the possibility of propagating the uncertainty between different stages of the analysis are among the main advantages probabilistic methods provide (Baker and Cornel 2008). Probabilistic analyses, though, often require making assumptions regarding the statistical distribution of the variables involved.

The lognormal distribution is frequently used to describe the statistical distribution of different demand parameters at discrete intensity levels or of the fragility function at distinct limit states (e.g. see e.g. Ibarra and Krawinkler 2005). The assumption of the lognormality of the data has been analyzed by several researchers, both for two-dimensional and for three-dimensional (3D) structural analysis (e.g. see Romao et al. 2011). In the latter case though, relevant results exist only for structural analyses that were performed with one angle of seismic incidence (ASI), where ASI is defined as the angle between the building's structural axes and the seismic action. Limited work has been done in probabilistic seismic analysis involving multiple ASIs, e.g. see the research by Lagaros (2010a) and (2010b), in which the lognormal data assumption was adopted in both studies.

In this context, the objective of the current study is twofold. Based on the results of 3D structural analyses performed considering multiple ASIs, the soundness of the lognormal statistical model is first examined when used to characterize the probability distribution of structural demand. Secondly, the performance of alternative statistical models to characterize the distribution of the structural demand is also evaluated. As such, the goodness of fit of seven statistical models, including the lognormal

[1]PhD student, CONSTRUCT-LESE, Faculty of Engineering, University of Porto, Portugal, dskoulidou@fe.up.pt
[2]PhD student, CONSTRUCT-LESE, Faculty of Engineering, University of Porto, Portugal, nmsp@fe.up.pt
[3]Assistant Professor, CONSTRUCT-LESE, Faculty of Engineering, University of Porto, Portugal, xnr@fe.up.pt

distribution, is analyzed when fitting them to demand samples. The performance of the statistical models is analyzed using quantile-quantile (Q-Q) plots whose assessment is performed visually and using the coefficient of determination R^2 of the corresponding linear regression. The results of these analyses highlight the influence of the ASI in probabilistic analysis and possible implications to the development of a statistical model of the demand needed for further risk or loss analyses.

2. METHODOLOGY AND STATISTICAL MODELS ANALYSED

The current study evaluates the performance of different statistical models to characterize the demand distribution obtained from 3D analyses when multiple ASIs are considered. Additionally, further insights are provided regarding the unconditional use of the lognormal model to represent seismic demand data. Six benchmark buildings are subjected to non-linear dynamic analysis for bi-directional ground motion groups of size n equal to 10, 15, 20, 25, 30, 35 and 40, applied along one to twelve ASIs. Two engineering demand parameters (EDP) are considered to represent seismic demand: maximum inter-story drift ratio (ISD) and maximum roof drift ratio (RD). The former is defined as the maximum ISD of the two structural directions, while the latter corresponds to the square root of the sum of squares (SRSS) combination of the displacements of two directions measured at the centre of mass. The probabilistic analysis is then performed for EDP samples obtained from discrete intensity levels (stripes) analyzed using ground motion groups of size n and a number of ASIs. In the following, the notation n_ASI will be used to refer to the results of a particular size n and number of ASIs.

Six statistical models are considered in addition to the lognormal distribution and are fitted to the EDP data of each sample. The distributions considered are the normal, the 2-parameter Weibull, the extreme value (EV), the Gamma, the generalized extreme value (GEV) and the Rayleigh. The GEV is a flexible three parameter model (location, scale, shape) that, depending on the shape parameter, can represent three different distribution families. The lognormal, Weibull, EV and GEV models are selected due to their suitability to characterize the distribution of maximum (extreme) values. The normal model is considered due to its widespread use in statistical analysis and also due to its performance for some types of demand data (e.g. see Romao et al. 2011). The Gamma distribution is considered given its flexibility to model different types of data. Finally, the Rayleigh model is often observed when the overall magnitude of a vector is related to its directional components.

The suitability of a probabilistic model to fit the sample data is usually checked using goodness-of-fit statistical tests, e.g. the Kolmogorov-Smirnov test. These tests are often developed to have power against specific distributions (D'Agostino and Stephens 1986), but their performance if often inadequate when small or very large sample sizes are examined, which is the case of the current study. Therefore, an alternative technique to assess the performance of the selected distributions to fit the data is applied herein. Goodness of fit is analyzed using Q-Q plots whose assessment is carried out by visual inspection and by computing the coefficient of determination R^2 that measures the adequacy of the linear fit between the empirical and the theoretical quantile data. An illustrative example of the procedure is presented in Figure 1 for an ISD sample and for two statistical models, the normal and the lognormal.

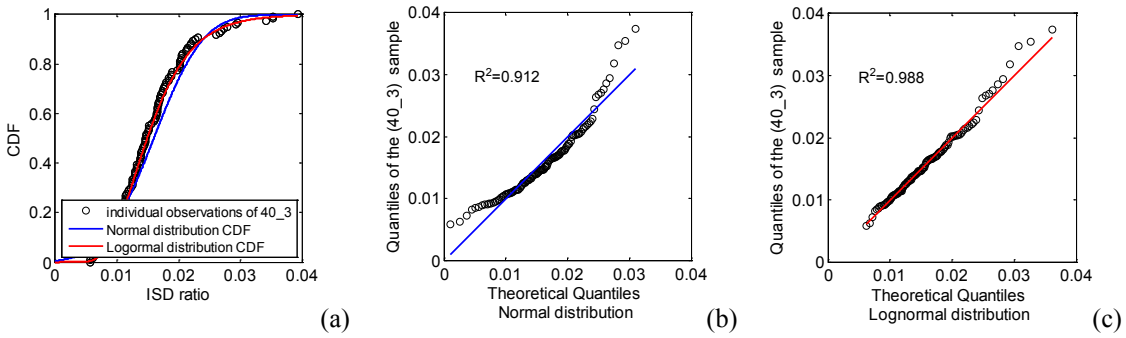

Figure 1. Cumulative distribution functions (CDF) of the normal and lognormal distributions fitted to a 40_3 ISD sample obtained for an intensity of 0.37g (a); Q-Q plots for the normal (b) and the lognormal (c) model.

The ISD sample corresponds to a 40_3 example obtained from the 5-story regular building (presented in Section 3.1) and for a seismic intensity equal to 0.37g (explained in Section 3.3). The cumulative distribution functions (CDFs) of the two statistical models fitted to the ISD sample are shown in Figure 1 (a). Figure 1 (b) and (c), represent the Q-Q plots for the normal and the lognormal model, respectively. The poor fitting of the normal model is evident from the plot and is further highlighted by the low R^2. On the other hand, the lognormal distribution exhibits a higher R^2 and provides a better fit to the data. Finally, it is noted that the purpose of the study is to examine the suitability of a given distribution family without making any assumptions regarding the parameters of the distributions.

3. DETAILS OF THE SELECTED BUILDINGS AND OF STRUCTURAL ANALYSES

3.1 Case studies and structural modeling

Six RC buildings with masonry infilled frame systems are analyzed. The selected buildings have configurations ranging from low- to mid-rise buildings with and without in-plan irregularities. Furthermore, all buildings are located in Lisbon, Portugal and are designed for gravity loads only. The plan view of a typical story of the 3-story irregular (3-Ir), the 4-story irregular (4-Ir) and the 5-story irregular (5-Ir) buildings is presented in Figure 2, along with design details. Similarly, in Figure 3, the plan view of a typical story of the 3-story regular (3-R), the 4-story regular (4-R) and the 5-story regular (5-R) buildings and the design details are also shown. The concrete strength and the yield strength of the reinforcing steel are equal to 25 MPa and 500 MPa, respectively.

All buildings are modeled in the OpenSees computer software (McKenna and Fenves 2011) considering mean values of the material and geometrical properties. A lumped plasticity approach is adopted to simulate the inelastic behavior of all structural elements. Phenomenological hysteresis laws are assigned in rotational springs located on both ends of all columns and beams to simulate inelastic flexural behavior. Two independent springs are assigned to each end of the columns, one for each orthogonal direction, while one spring is assigned to each end of the beams modeling the in-plane flexural behavior. Due to the nature of the selected inelastic modeling approach, no bi-axial moment interaction or axial force moment interaction is considered when modeling the behavior of columns. Hysteretic flexural behavior is simulated using the *hysteretic* material provided by OpenSees. The yielding strength (M_y) and the yielding rotation capacity (θ_y) are determined according to Panagiotakos and Fardis (2001). The capping (θ_c) and post-capping rotation (θ_{pc}) capacities are computed according to Haselton et al. (2008) and a final 20% residual strength (M_r) is considered at the ultimate rotation capacity (θ_u) (see the backbone curve in Figure 4(a)).

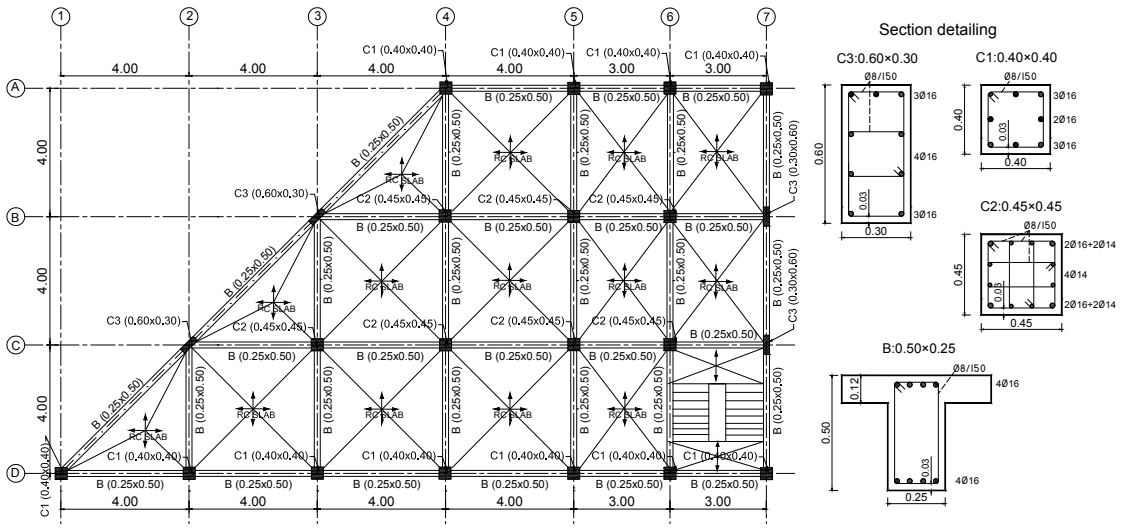

Figure 2. Plan view of a typical story of the 3-Ir, 4-Ir and 5-Ir buildings and design details.

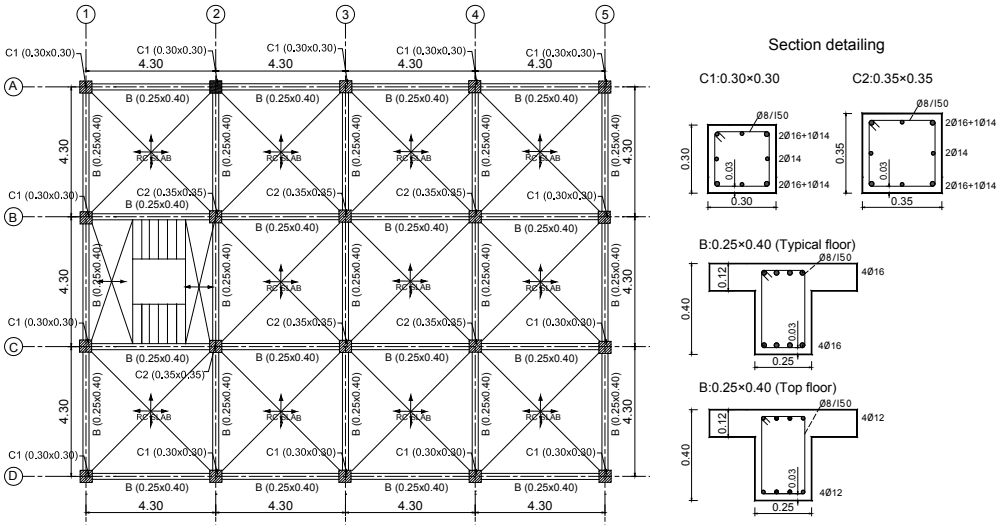

Figure 3. Plan view of a typical story of the 3-R, 4-R and 5-R buildings and design details.

Stiffness, strength and unloading stiffness degradations are considered in the hysteresis curves. Each beam-column element is defined by a serial arrangement of the end springs connected to a linear elastic element. A stiffness modification factor equal to 10 is applied according to Ibarra and Krawinkler (2005) and Zareian and Medina (2010) to account for the effect of the series connection of the elements on the total stiffness of the element. For the beam-column joint, rigid elastic elements are considered with a length equal to half of the length of the corresponding perpendicular element. The possibility of shear failure or beam-column joint failure is not modelled but can be analyzed in post-processing.

Infills are considered in all peripheral frames and are modelled using two diagonal compression only strut elements. The equivalent area of each strut is established based on the maximum lateral force of the infill and on the masonry compressive strength (Dolšek and Fajfar 2008). The parameters obtained, i.e. the maximum stress (f_m) and strain, are used to define the masonry material with zero tensile strength simulated by the *Concrete01* constitutive model (Figure 4 (b)). The masonry compressive strength is equal to 3.10 MPa and all infills have a thickness of 0.15m. Additionally, a residual stress equal to 10% of the maximum stress is considered for numerical stability.

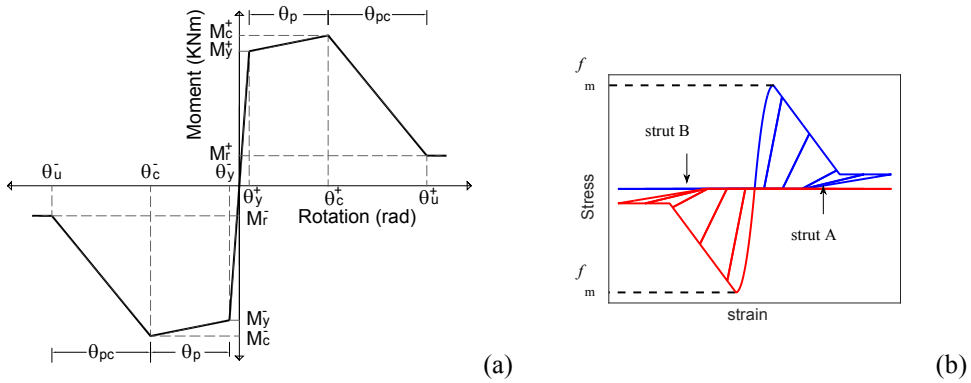

Figure 4. Backbone curve of the Moment-Rotation relationship of all structural elements (a) and cyclic behavior of the strut material of the infills.

A permanent load of 4 kN/m^2 is uniformly distributed on all slabs, additional to the slab self-weight. A uniform live load of 3 kN/m^2 is also assigned to all slabs, except to the top story slabs, where the live load is 1 kN/m^2. Staircases are modeled only as permanent and live loads, which are transferred to the

supporting beams and applied uniformly. The corresponding loads are 7.75 kN/m and 8.60 kN/m for the permanent and the live loads, respectively. Masonry infills also load uniformly all peripheral frames with 7 kN/m. The fundamental periods of vibration of each structure are presented in Table 1.

Table 1. Periods of vibration of the studied buildings.

Periods (s)	**3-R**	**4-R**	**5-R**	**3-Ir**	**4-Ir**	**5-Ir**
T_1,T_2 (w infills)	0.31, 0.25	0.41, 0.31	0.52, 0.39	0.21, 0.15	0.29, 0.20	0.37, 0.26
T_1,T_2 (w/o infills)	0.73, 0.72	0.96, 0.93	1.18, 1.15	0.39, 0.35	0.55, 0.47	0.70, 0.60

3.2 Ground motion selection

The ground motion selection is carried out using the recently developed SelEQ software (Macedo and Castro 2017) considering a conditional mean spectrum (CMS) (Baker 2010) as the target spectrum. The probabilistic seismic hazard analysis of the site is first performed using OpenQuake (Pagani et al. 2014) considering Lisbon, Portugal, as the benchmark site for all structures. Hazard disaggregation is then carried out for four probabilities of exceedance, i.e. 50%, 10%, 5% and 2% in 50 years, at a value of T* for each building. Four CMS are subsequently constructed for each building, each one associated with one of the probabilities of exceedance. The structural period T* corresponds to the average of the first two periods of the building with the infills and the first two periods of the building without the infills (see Table 1). Involving the periods of vibration of the bare structure in the definition of T* is conceptually similar to accounting for the period elongation of the structure after yielding and failure of the infills. Figure 5 shows the four CMS for the 5-R building that has T*=0.82s.

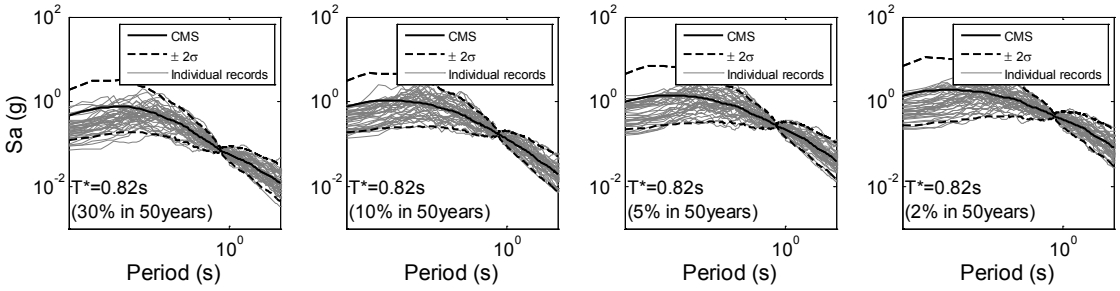

Figure 5. The CMS and the geometric means of the 40 ground motions for the 5-R building.

Ground motion selection is based on a preliminary selection of ground motions from the NGA database (Akkar et al. 2014) based on seismological and strong motion parameters. Subsequently, using the CMS as a target spectrum, 40 bi-directional ground motion records are selected implementing the criteria and the objective function described in Macedo and Castro (2017). As a result, four groups of 40 bi-directional ground motions are obtained for each building, one for each CMS corresponding to the previously referred probabilities of exceedance of 50%, 10%, 5% and 2% in 50 years, e.g. see Figure 5 for the case of the 5-R building and T*=0.82 s.
Each group of 40 bi-directional records is subsequently re-sampled to create groups of size n = 10, 15, 20, 25, 30 and 35. Specific provisions are considered to maintain the compatibility between each new group and the reference group of size 40 in terms of seismic input. As a result, a total number of 100 groups are obtained for each size n.

3.3 Probabilistic demand model and uncertainty considerations

The six buildings presented in Section 3.1 are subjected to multi-stripe analysis (MSA) (Jalayer and Cornell 2009) with the ground motion groups defined in Section 3.2. Following a procedure similar to the one proposed by Christovasilis et al. (2014), the four groups, corresponding to the intensities associated to the previously referred probabilities of exceedance, are scaled up and down to cover a total of fifteen intensities. Figure 6 shows a schematic representation of the scaled average geometric

response spectra for the case of the 5-R building (T*=0.82s) and the corresponding scale factors.

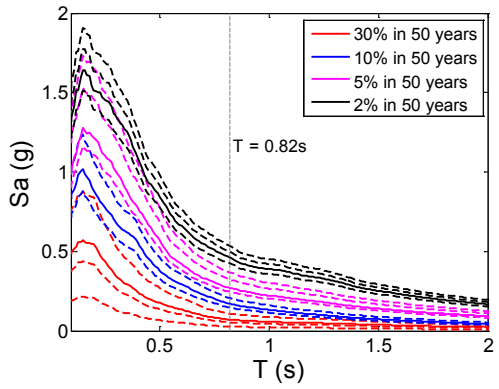

Probability of exceedance	Scale factor	Sa(T*=0.82) (g)
30% in 50 years	0.40	0.03
	0.67	0.05
	1.00	0.07
	1.48	0.11
10% in 50 years	0.82	0.14
	1.00	0.17
	1.23	0.21
5% in 50 years	0.90	0.24
	1.00	0.27
	1.21	0.32
	1.39	0.37
2% in 50 years	0.91	0.42
	1.00	0.46
	1.09	0.50
	1.17	0.54

Figure 6. Average geometric response spectra of the 40 ground motions for different intensities (left) and the scale factors (right) for the 5-R building (T*=0.82s).

All six buildings are subsequently subjected to nonlinear time history analyses for the fifteen intensity levels (stripes) with the 40 record pairs of each stripe applied along twelve ASIs. The considered ASIs range from 0° to 165° in steps 15° and are considered to be equally likely. The sources of uncertainty considered in the structural response are therefore the result of the record-to-record variability and the ASI of each record. As referred in Section 3.2, 100 groups of ground motions are created for each size n of ground motions to take into account the record-to-record variability in different group sizes. All groups are also applied along different number of ASIs, from one to twelve. The ASIs are sampled from a uniform distribution and a total of 100 combinations of ASIs of size one to twelve are considered. Table 2 summarizes the analyzed cases.

Table 2. Analyzed cases (gr. stands for groups).

ASI \ n	10	15	20	25	30	35	40
1	100 gr	100 gr.	100 gr.	100 gr.	100 gr.	100 gr.	1 gr.
2	100 gr.	100 gr.	100 gr.	100 gr.	100 gr.	100 gr.	1 gr.
…	…	…	…	…	…	…	…
11	100 gr.	100 gr.	100 gr.	100 gr.	100 gr.	100 gr.	1 gr.
12	100 gr.	100 gr.	100 gr.	100 gr.	100 gr.	100 gr.	1 gr.

4. RESULTS AND DISCUSSION

Figure 7 shows the Q-Q plots and corresponding R^2 values of the ISD data obtained from the analysis of the 5-R building, for one group of 35_4 and for an intermediate ground motion intensity level (Sa(T*)=0.24g). As can be seen, the lognormal and the GEV distributions appear to be the more adequate, followed by the Gamma distribution. The normal and the Weibull distributions demonstrate weaker fits when compared to the previously referred distributions, while the Rayleigh and the EV distribution fits exhibit very low performance. Due to their poor fitting in most of the cases that were analyzed, results from the Rayleigh and the EV distributions will be omitted hereon.
Figure 8 to Figure 11 show the average R^2 values (average of the 100 groups of records of a size n and a given number of ASIs) for all buildings and for all the selected n_ASI combinations. Specifically, the 35_1 and 35_12 results of the ISD and RD are presented in Figure 8 and Figure 9, respectively. Likewise, the 15_1 and 15_12 results of the ISD and the RD are presented in Figure 10 and Figure 11, respectively. The results obtained from the groups of size n=35 are representative of larger group sizes (n≥25), while the results obtained from the groups of size n=15 are representative of smaller group

sizes ($n \leq 20$). Given the expected dependence of R^2 on the sample size of the fitted data, the results should be interpreted separately for each n_ASI combination and the focus should be given to the relative variations of R^2 among the different distributions.

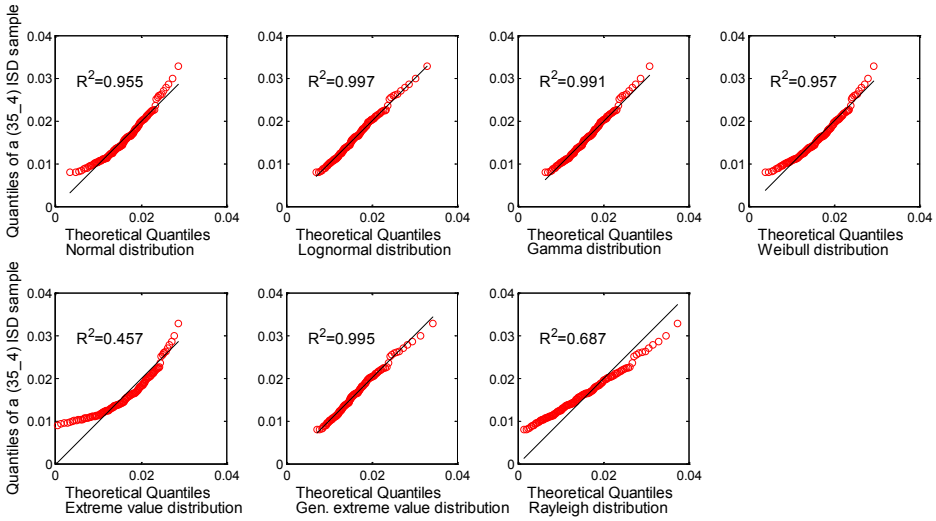

Figure 7. Q-Q plots and corresponding R^2 values of all considered distributions for a 35_4 ISD sample that corresponds to inelastic response of the 5-R building.

It is observed that the GEV presents the best fitting for most of the cases of all buildings, number of ASIs and intensity level, followed closely by the lognormal distribution. This trend holds true for both the ISD and the RD. The Gamma distribution also presents good fitting performance, sometimes even superior to the two previously referred distributions; e.g. see the 15_1 ISD fitting of the 3-Ir building for the elastic response (Figure 10). Still, the differences can be characterized as negligible. The adequacy of the normal and the Weibull distributions can be seen to vary considerably, depending on the building height and regularity and on the level of inelasticity. It can be further observed that the number of ASIs involved does not seem to significantly affect the type of the statistical model that best fits the demand distribution. On this respect, the smallest variations can be seen in the elastic response of the buildings and for the RD, while the largest variations are found for the mainly inelastic response and for the ISD.

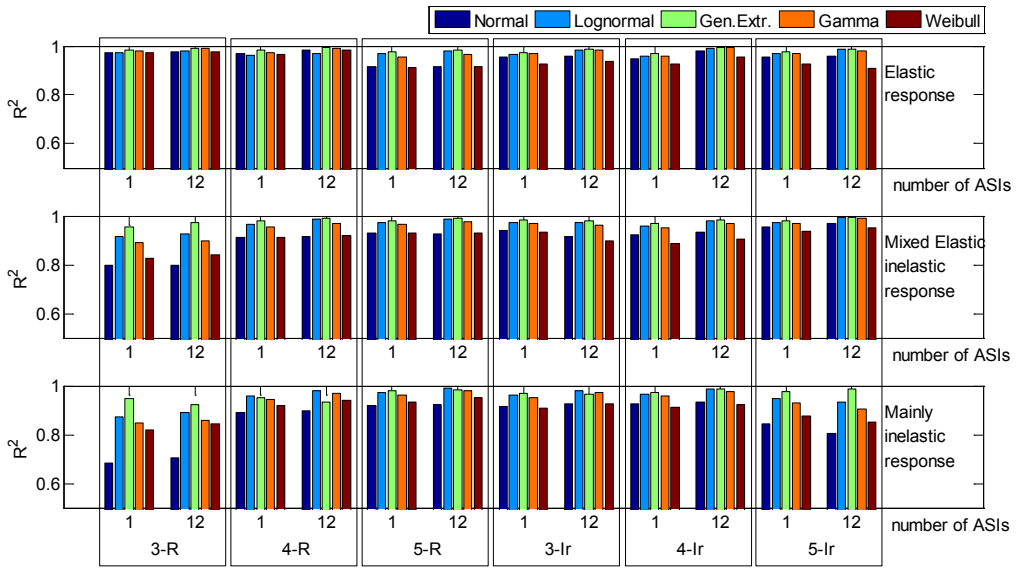

Figure 8. Average R^2 obtained from ISD Q-Q plots for 35_1 and 35_12 for all buildings.

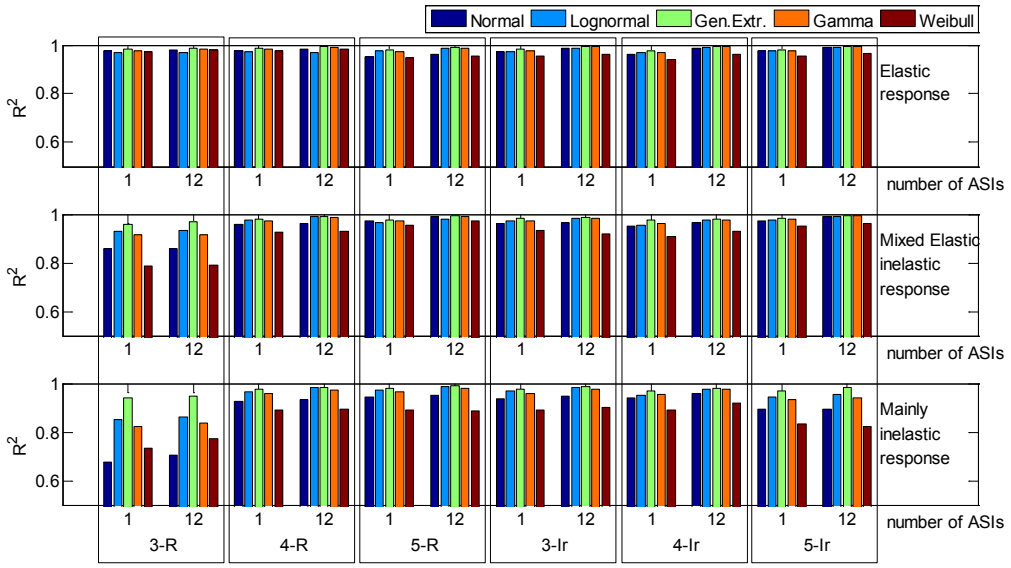

Figure 9. Average R^2 obtained from RD Q-Q plots for 35_1 and 35_12 for all buildings.

Focusing on the results for size n=35 (Figure 8 and Figure 9), the GEV distribution seems to provide the best fit for both EDPs and for all levels of inelasticity. An exception to this trend can be seen for the ISD of the 4-R, 5-R and 3-Ir buildings and for the mainly inelastic response, where the lognormal distribution appears to fit better. The coefficient of variation (cov) of R^2 for the 100 groups and for both distributions is always lower than 5%, except for one case of the lognormal distribution where it is 6.6%. Also, apart from the cases where the lognormal distribution provides a better fit to the data, the cov of the GEV is lower than the cov of the lognormal distribution.

As opposed to the consistent trends observed for the larger group sizes, the results obtained for the smaller group sizes (shown in Figure 10 and Figure 11) are characterized by a larger variability that also increases as the intensity level increases. Focusing on the mainly inelastic response of Figure 10 and Figure 11, it can be seen that a consistent trend is not observed and that the distribution exhibiting better performance constantly changes between the GEV and the lognormal distribution.

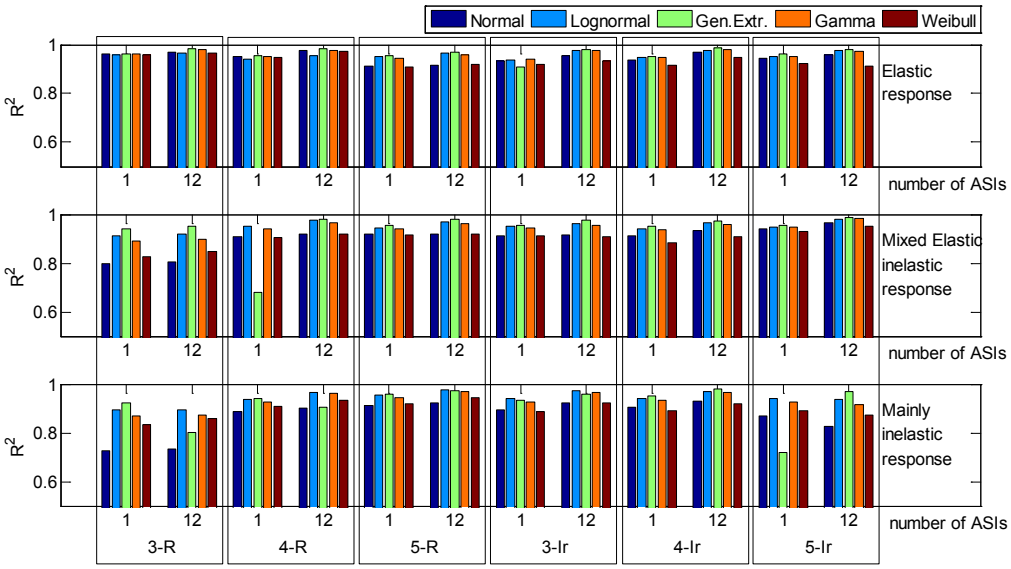

Figure 10. Average R^2 obtained from ISD Q-Q plots for 15_1 and 15_12 for all buildings.

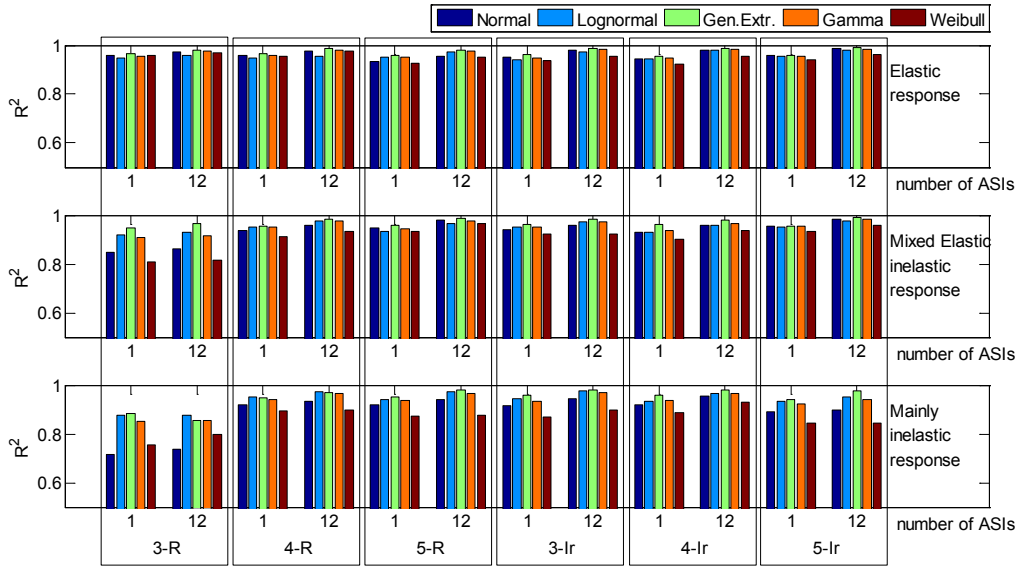

Figure 11. Average R^2 obtained from RD Q-Q plots for 15_1 and 15_12 for all buildings.

Additionally, the cov of R^2 obtained for the groups of size n=15 is always larger when compared to the value obtained for groups of size n=35. Furthermore, the GEV distribution presents higher covs when compared to the covs of the lognormal distribution for most buildings and for both EDPs. More specifically, the larger values of cov are found in all cases where the GEV yields a significantly low R^2 due to its inability to provide a good fit to the data. The initial fitting is performed using the maximum likelihood method with 400 iterations and a tolerance of 10e-5. However, no better performance could be achieved by changing the tolerance or by increasing the number of iterations. These cov values may reach up to 40%, indicating a large variability.

In order to demonstrate the evolution of R^2 between the different distribution models when more numbers of ASIs are used, the R^2 values are aggregated over all buildings, and an average R^2 value is obtained for each statistical model and plotted in Figure 12 to Figure 15. Furthermore, two group sizes n are considered for both EDPs and correspond to 30, shown in Figure 12 and Figure 13, and 20, shown in Figure 14 and Figure 15.

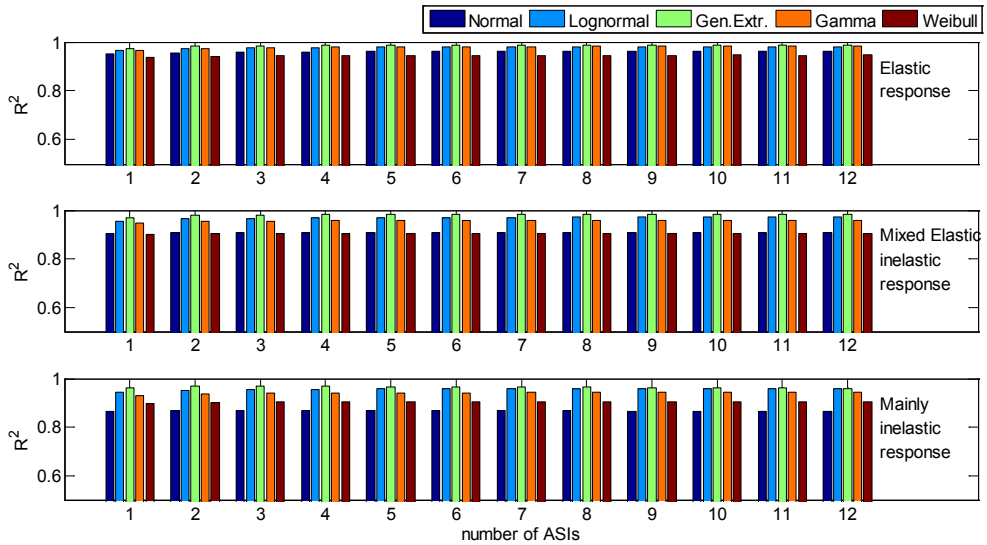

Figure 12. Average R^2 of all buildings obtained from ISD Q-Q plots for ASIs 1 to 12 and for n = 30.

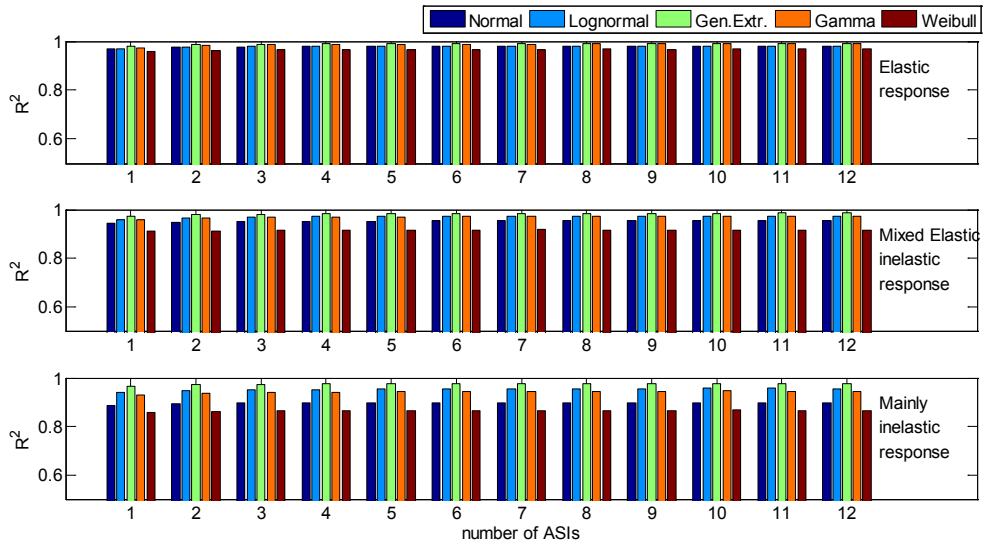

Figure 13. Average R^2 of all buildings obtained from RD Q-Q plots for ASIs 1 to 12 and for n = 30.

The superior performance of the GEV is apparent in most of the cases shown in Figure 12 to Figure 15. The analysis with more than 1 ASI doesn't seem to affect the type of model representing the demand distribution of the RD in any intensity level. The same trend can be observed for the ISD distribution when the response is elastic and mixed elastic/inelastic. On the contrary, when the response is mainly inelastic, considering more than 1 ASIs seems to favor the use of the lognormal over the GEV distribution. The latter observation is particularly obvious for the smaller ground motion group size (see Figure 14).

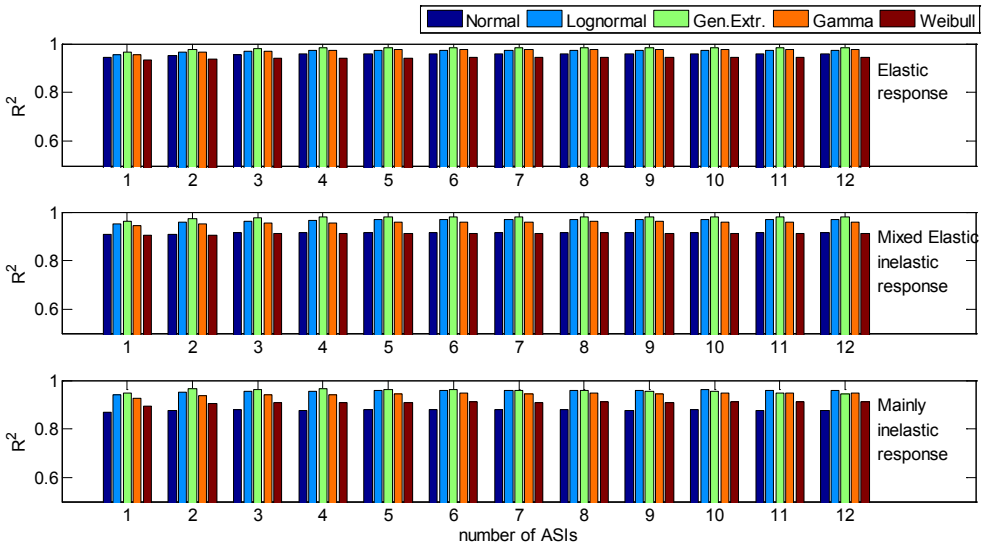

Figure 14. Average R^2 of all buildings obtained from ISD Q-Q plots for ASIs 1 to 12 and for n = 20.

Overall, it is observed that the GEV distribution presents a better fitting performance for most of the cases when the ground motion size is large enough ($n \geq 25$). Still in the case of larger group sizes, and for inelastic response, the fitting of the GEV is superior to the lognormal given the smaller R^2 cov values that were observed. On the other hand, when small group sizes are considered ($n \leq 20$), the cov of the GEV fittings increases considerably indicating its inadequacy in several cases. The lognormal distribution, despite featuring a lower fitting performance than the GEV, seems to provide much more

stable fittings and thus a more reliable performance. At the same time, the average R^2 values of the lognormal distribution are over 90% regardless of the number of ASIs and the covs of the R^2 are rarely above 10%.

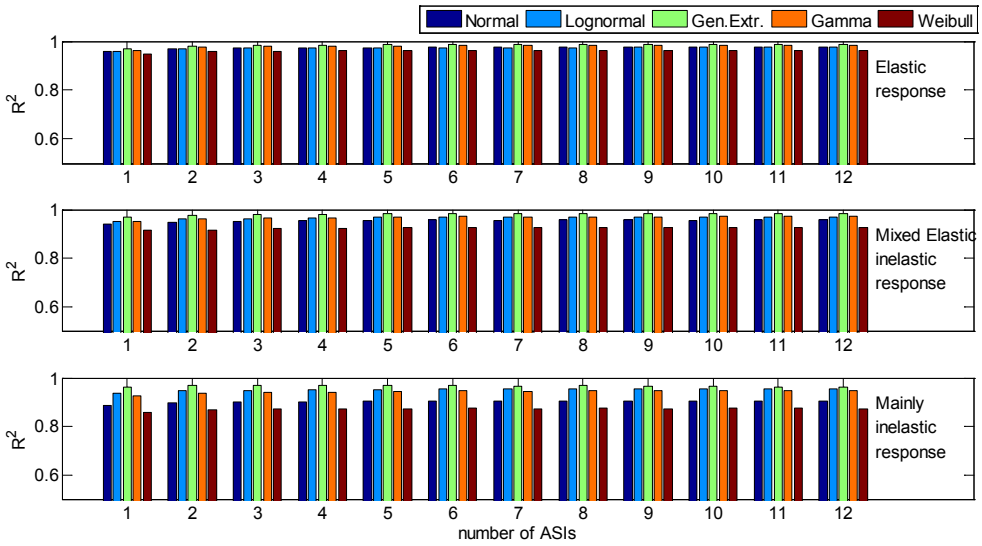

Figure 15. Average R^2 of all buildings obtained from RD Q-Q plots for ASIs 1 to 12 and for n = 20.

As a final remark, despite the overall better performance of the GEV distribution to characterize the demand distribution when one or more ASIs are taken into account when compared to the lognormal distribution, two factors render its use less efficient. First, the difficulty in fitting the GEV to the data when small ground motion groups are used, especially for higher seismic intensities. Second, the fact that three parameters are required to fully characterize the GEV distribution. Instead, the lognormal distribution, although exhibiting marginally lower performance, has a stable and low cov even when a low number of ground motions is used. Finally, only two parameters are required to fully characterize the lognormal distribution and thus it can be is the best option even when more than one ASI is used.

5. CONCLUSIONS

The effect of the ASI on the probabilistic seismic demand of RC buildings is examined, in particular the influence of the selected number of ASIs in the type of statistical distribution that is used to fit seismic demand and develop with a probabilistic model. Six RC buildings are analyzed for different numbers of ground motion groups applied along one to twelve ASIs and for fifteen intensity levels. Seven statistical models are fitted to the demand observations for all cases and the performance of each model is evaluated through Q-Q plots and the corresponding R^2. The distribution of both the ISD and the RD is tested.

The R^2 comparisons show that the Rayleigh and the EV models are inappropriate to characterize the demand distribution of both EDPs. Moreover, the normal and the Weibull distributions exhibit low fitting performance that is also characterized by significant variability when fitting highly inelastic structural response. The Gamma distribution shows an adequate fitting performance for all cases, but inferior to that of the lognormal and the GEV distributions. The GEV presents the best fitting performance in most of the cases. However, this performance exhibits a high variability when ground motion group sizes lower than 25 are used, particularly for larger intensity levels. The lognormal distribution, on the other hand, shows a more stable behavior. Based on its low variability and on the fact that is characterized by only two parameters, the lognormal distribution is considered the best model to represent the demand distribution of both EDPs studied herein, when more than one ASIs are used.

6. ACKNOWLEDGMENTS

The first author would like to acknowledge the financial support from the Foundation of Science and Technology (FCT) of Portugal through the grant PD/BD/113681/2015. The authors would also like to acknowledge the assistance of Luis Macedo who provided the seismic hazard results and the ground motion records.

7. REFERENCES

Akkar S, Sandıkkaya MA, Şenyurt M, Sisi AA, Ay BÖ, Traversa P, Douglas J, Cotton F, Luzi L, Hernandez B, Godey S (2014). Reference database for seismic ground-motion in Europe (RESORCE). *Bulletin of earthquake engineering*, 12(1): 311-339.

Baker JW (2010). Conditional mean spectrum: Tool for ground-motion selection. *Journal of Structural Engineering*, 137(3): 322-331.

Baker JW, Cornell CA (2008). Uncertainty propagation in probabilistic seismic loss estimation. *Structural Safety*, 30(3): 236-252.

Christovasilis IP, Cimellaro GP, Barani S, Foti S (2014). On the selection and scaling of ground motions for fragility analysis of structures. *Proceedings of the 2nd European Conference on Earthquake Engineering and Seismology*, 24-29 August, Istanbul, Turkey.

D'Agostino RB, Stephens MA (1986). Goodness-of-fit techniques (Statistics, a series of textbooks and monographs). Dekker, 68, 1.

Dolšek M, Fajfar P (2008). The effect of masonry infills on the seismic response of a four-storey reinforced concrete frame - a deterministic assessment. *Engineering Structures*, 30(7): 1991-2001.

Haselton CB, Goulet CA, Mitrani-Reiser J, Beck JL, Deierlein GG, Porter KA, Taciroglu E (2008). An assessment to benchmark the seismic performance of a code-conforming reinforced-concrete moment-frame building. *Pacific Earthquake Engineering Research Center*, (2007/1).

Ibarra LF, Krawinkler H (2005). Global collapse of frame structures under seismic excitations. Peer report 2005/2006. Berkeley, CA: Pacific Earthquake Engineering Research Center.

Jalayer F, Cornell CA (2009). Alternative non-linear demand estimation methods for probability-based seismic assessments. *Earthquake Engineering & Structural Dynamics*, 38(8): 951-972.

Lagaros ND (2010a). Multicomponent incremental dynamic analysis considering variable incident angle. *Structure and Infrastructure Engineering*, 6(1-2): 77-94.

Lagaros ND (2010b). The impact of the earthquake incident angle on the seismic loss estimation. *Engineering Structures*, 32(6): 1577-1589.

Macedo L, Castro JM (2017). SelEQ: An advanced ground motion record selection and scaling framework. *Advances in Engineering Software*. 114 (2017): 32–47.

McKenna F, Fenves GL (2011). Opensees 2.5.0, Computer Software. UC Berkeley, Berkeley (CA). http://opensees.berkeley.edu

Pagani M, Monelli D, Weatherill G, Danciu L, Crowley H, Silva V, Henshaw P, Butler L, Nastasi M, Panzeri L, Simionato M (2014). OpenQuake engine: an open hazard (and risk) software for the global earthquake model. *Seismological Research Letters*, 85(3): 692-702.

Panagiotakos TB, Fardis MN (2001). Deformations of reinforced concrete members at yielding and ultimate. *Structural Journal*, 98(2): 135-148.

Romao X, Delgado R, Costa A (2011). Assessment of the statistical distributions of structural demand under earthquake loading. *Journal of Earthquake Engineering*, 15(5): 724-753.

Zareian F, Medina RA (2010). A practical method for proper modeling of structural damping in inelastic plane structural systems. *Computers & structures*, 88(1): 45-53.